LETTERS
https://doi.org/10.1038/s41565-017-0043-5
nature nanotechnology

A modular platform for targeted RNAi therapeutics

Ranit Kedmi[1], Nuphar Veiga[1], Srinivas Ramishetti[1], Meir Goldsmith[1], Daniel Rosenblum[1], Niels Dammes[1], Inbal Hazan-Halevy[1], Limor Nahary[2], Shani Leviatan-Ben-Arye[1], Michael Harlev[3], Mark Behlke[4], Itai Benhar[2], Judy Lieberman[5] and Dan Peer[1]*

Previous studies have identified relevant genes and signalling pathways that are hampered in human disorders as potential candidates for therapeutics. Developing nucleic acid-based tools to manipulate gene expression, such as short interfering RNAs[1–3] (siRNAs), opens up opportunities for personalized medicine. Yet, although major progress has been made in developing siRNA targeted delivery carriers, mainly by utilizing monoclonal antibodies (mAbs) for targeting[4–8], their clinical translation has not occurred. This is in part because of the massive development and production requirements and the high batch-to-batch variability of current technologies, which rely on chemical conjugation. Here we present a self-assembled modular platform that enables the construction of a theoretically unlimited repertoire of siRNA targeted carriers. The self-assembly of the platform is based on a membrane-anchored lipoprotein that is incorporated into siRNA-loaded lipid nanoparticles that interact with the antibody crystallizable fragment (Fc) domain. We show that a simple switch of eight different mAbs redirects the specific uptake of siRNAs by diverse leukocyte subsets in vivo. The therapeutic potential of the platform is demonstrated in an inflammatory bowel disease model by targeting colon macrophages to reduce inflammatory symptoms, and in a Mantle Cell Lymphoma xenograft model by targeting cancer cells to induce cell death and improve survival. This modular delivery platform represents a milestone in the development of precision medicine.

Targeted drug delivery to diseased cells reduces bystander cell toxicity and can be used to transport poorly permeable drugs, such as nucleic acid-based therapeutic molecules[1–3]. Active cellular targeting carriers that encapsulate siRNAs were shown to promote effective gene silencing. Clinical studies using lipid-based nanoparticles (LNPs) that carry siRNA payloads or GalNAc-conjugated siRNAs that are taken up by the asialoglycoprotein receptor on hepatocytes are showing impressive and durable gene knockdown in the liver in advanced phase trials[1–3]. Although designing useful strategies for delivering siRNAs to cells outside the liver, such as leukocytes, has proven difficult, by utilizing antibodies as fusion proteins or conjugated to LNPs, we and others were able to demonstrate specific gene knockdown in murine lymphocytes[4–8]. These studies support the development of targeted siRNA delivery platforms for therapeutics of leukocyte-based diseases, such as autoimmune diseases and cancer.

Inflammatory conditions and cancer are multifactorial diseases and an optimal therapy will target different gene targets in distinct cell types. A wide variety of targeted delivery carriers that utilize diverse targeting moieties is required due to the heterogeneities in cancer. Individuals differ in the profiles of their cancer cell surface receptors, and the variance within tumour cell populations is also high. Thus, an effort to eradicate cancer by targeting a single receptor will most probably fail and cause resistant cancer cells to flourish once deprived of this specific targeted receptor. Therefore, a delivery platform that can be adjusted for each patient and target several receptors would be ideal. However, constructing a wide variety of targeted delivery platforms is not feasible with current methodologies. Although mAbs that bind with high affinity and selectivity to cell-specific receptors are broadly available, the chemical conjugation of those mAbs, which differ in their amino-acid composition, to LNPs is inefficient and requires careful optimization for each mAb[4–8].

Here, we developed a flexible platform for cell-specific siRNA delivery that can be easily customized, with no need for further development, to target any cell receptor. The LNPs are non-covalently coated with targeting antibodies via a recombinant protein (anchored secondary scFv enabling targeting, named ASSET). ASSET is a membrane-anchored lipoprotein that is incorporated into siRNA-loaded lipid nanoparticles and interacts with the antibody Fc domain. For this purpose, ASSET is composed of two functional domains—an N-terminal signal sequence followed by a short CDQSSS peptide NlpA motif that undergoes lipidation in bacteria and an scFv of a monoclonal antibody (clone RG7/1.30)[9] that binds to the Fc constant region of Rat IgG2a antibodies (Fig. 1a–c, Supplementary Fig 1). This lipidation strategy, previously used for displaying proteins anchored to the inner membrane of *Escherichia coli*[10,11], allows the purified recombinant lipidated ASSET to be inserted into any lipid vesicle. An mCherry domain and His-tag were fused to the C terminus of ASSET to enable us to track cell uptake of ASSET-coated LNPs and for ASSET purification, respectively.

ASSET was expressed and purified from bacteria with a high yield (30 mg l^{-1}) and purity of ~47.5% (Fig. 1d) with minimal endotoxin contamination (1.57 endotoxin units per kg). Purified mutated (m)

[1]Laboratory of Precision NanoMedicine, School of Molecular Cell Biology and Biotechnology, George S. Wise Faculty of Life Sciences, Department of Materials Sciences and Engineering, Iby and Aladar Fleischman Faculty of Engineering, Center for Nanoscience and Nanotechnology, Cancer Biology Research Center, Tel Aviv University, Tel Aviv, Israel. [2]School of Molecular Cell Biology and Biotechnology, Department of Molecular Microbiology and Biotechnology, George S. Wise Faculty of Life Sciences, Tel Aviv University, Tel Aviv, Israel. [3]Veterinary Service Center, Sackler Faculty of Medicine, Tel Aviv University, Tel Aviv, Israel. [4]Integrated DNA Technologies Inc., Coralville, IA, USA. [5]Program in Cellular and Molecular Medicine, Boston Children's Hospital, and Department of Pediatrics, Harvard Medical School, Boston, MA, USA. R.K. and N.V. contributed equally to this work. *e-mail: peer@tauex.tau.ac.il

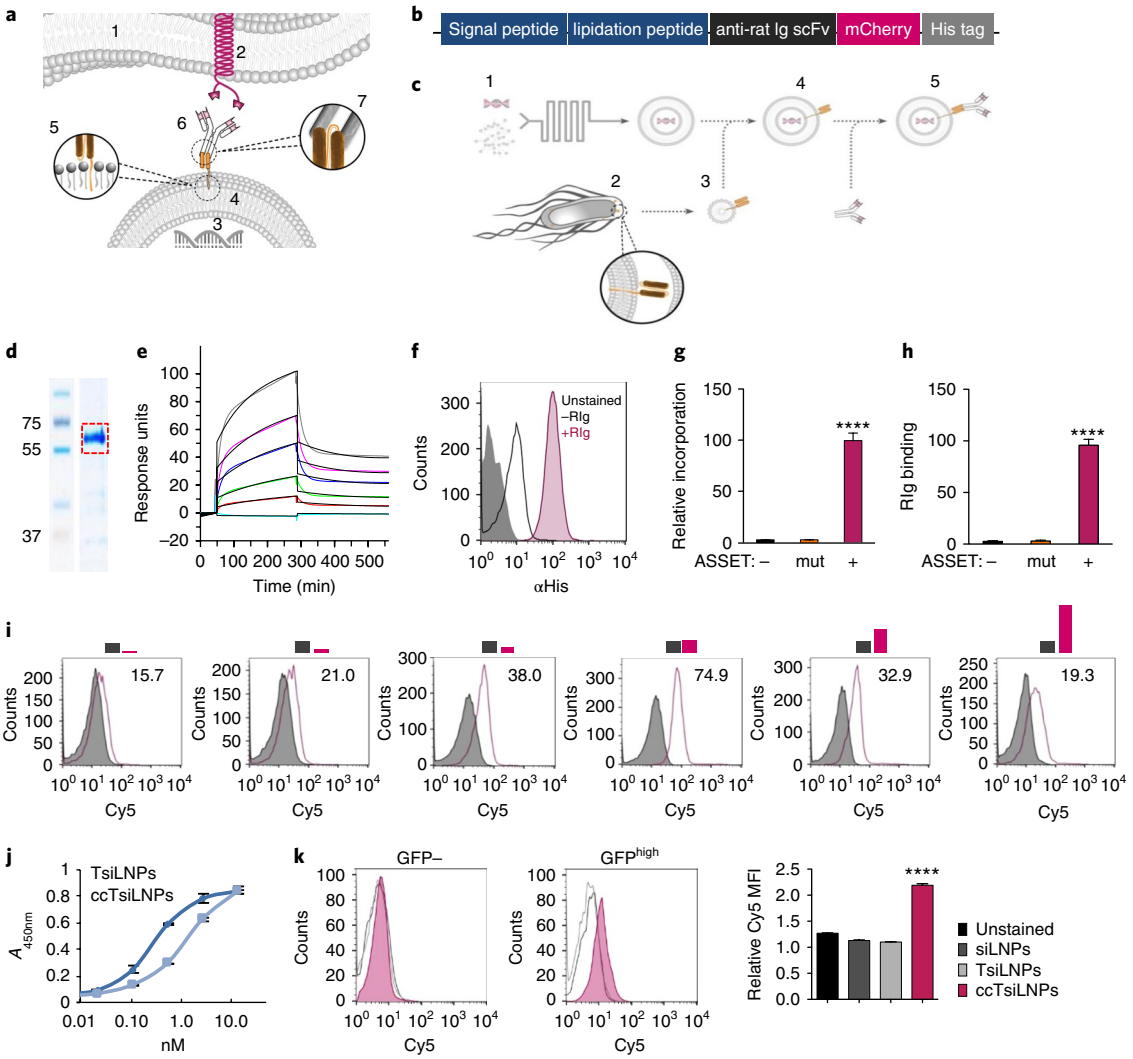

Fig. 1 | ASSET platform design and construction. a, Schematic illustration of ASSET incorporation into LNPs, binding to RIg and targeting. 1, Target cell membrane; 2, targeted cell-surface receptor; 3, encapsulated siRNA; 4, LNP; 5, ASSET anchored in the LNP; 6, RIg; 7, interaction between ASSET scFv and RIg Fc. **b**, ASSET expression vector. **c**, TsiLNP construction. Microfluidic mixing of lipids and siRNA resulted in siLNPs (1). ASSET, expressed in the *E. coli* periplasm anchored by lipidation to the inner membrane (2), is purified in micelles (3); inserted into the siLNP (4) and coated with RIg (5). **d**, Cropped polyacrylamide/SDS gel electrophoresis of purified ASSET stained with Coomassie blue. The red box indicates ASSET. Lanes were cropped from the same gel. **e**, Mutated mASSET (0 (light blue), 3 (red), 6 (green), 12 (blue), 18 (purple), and 30 (brown) nM) binding to RIg as assessed by Biacore using immobilized RIg. Black lines represent fits to the kinetic model. **f**, Representative flow histograms to measure binding of purified ASSET to TK1 cells that were pre-incubated (red) or not (black) with αLFA-1 RIg. Untreated cells are shaded grey. ASSET was detected by αHis. **g**,**h**, Incorporation of ASSET (+) or lipidation-defective mASSET into LNPs as quantified by mCherry fluorescence determined by the fluorescence remaining in TsiLNPs after dialysis to remove unbound protein (**g**) or assessed by ELISA after dialysis to remove unbound protein (**h**). **i**, Uptake of Cy5-siRNA-loaded αLFA-1 TsiLNPs, constructed using the indicated molar ratios of ASSET:RIg, into TK1 cells as assessed by flow cytometry measurements of Cy5 mean fluorescence intensity (MFI) (red). Uncoated TsiLNPs lacking RIg served as a negative control (grey). The molar ratios are shown in the grey and red boxes for ASSET and Rig respectively. **j**, The CD34 binding affinity of αCD34 RIg incorporated in TsiLNPs or ccTsiLNPs as assayed by ELISA. **k**, HEK293T cells were transiently transfected with rat Fc receptor and GFP. Representative flow histograms measure the binding of Cy5-siRNA-loaded αCD34 TsiLNPs (grey), αCD34 ccTsiLNPs (red) and untargeted siLNPs (dark grey) to transfected HEK293T gated for GFP^{high}, and to untransfected cells gated for GFP-. Right: mean ± s.d. ratio of Cy5 MFI of GFPhigh and GFP–, normalized to siLNP binding. Data in **d**–**k** are representative of 3 independent experiments; data in **g**, **h** and **k** are the mean ± s.d., $n = 3$. ****$P < 0.0001$ (two-sided student's t-test).

ASSET, composed of a fusion protein containing a mutated NlpA motif, specifically bound to Rat IgG2a (RIg) with a dissociation constant K_d of ~22.7 nM as measured in three independent replicates by surface plasmon resonance (SPR) (Fig. 1e) and selectively bound to cells coated with RIg compared with uncoated cells (Fig. 1f). When ASSET was incubated with LNPs, it was incorporated, as quantified by mCherry fluorescence (Fig. 1g) and enzyme-linked immunosorbent assay (ELISA) (Fig. 1h) in three independent repeats with 99.6% and 95.8% efficiency, respectively. Incorporation required the NlpA lipidation motif as mASSET was not incorporated into LNPs. Lipidation therefore directed ASSET anchoring.

ASSET incorporation slightly increased the size of the LNP from 66 ± 11 to 75 ± 14 nm and the polydispersity index (PDI) from 0.10 to 0.16 by dynamic light scattering (Supplementary Table 1). These particles retained both their spherical shape (Supplementary Fig 2a) and efficient siRNA loading (Supplementary Fig 2b), even after a

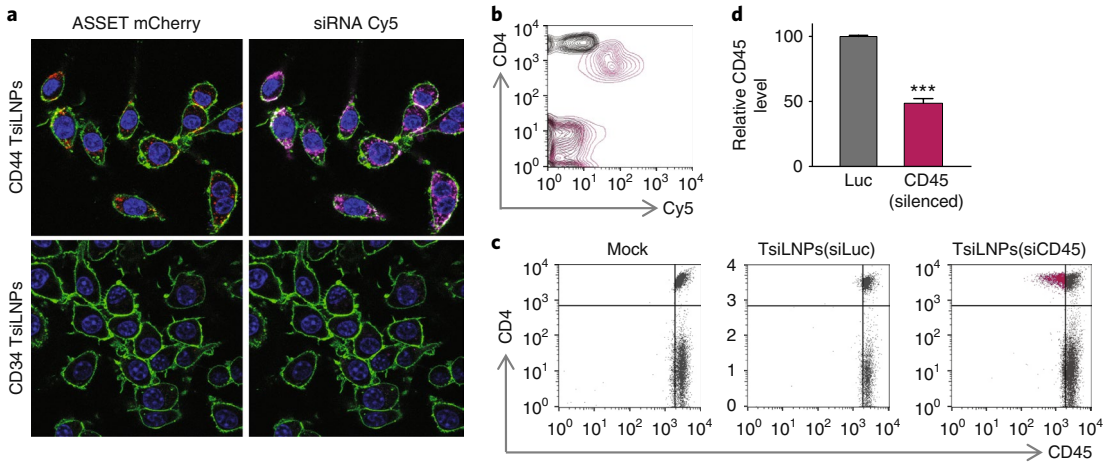

Fig. 2 | TsiLNP functionality in vitro and in vivo. a, Confocal microscopy of CD44 + CD34- RAW 264.7 cells incubated with Cy5-siRNA-loaded αCD44 or αCD34 TsiLNPs. LNP incorporation was visualized by Cy5 or mCherry (red); nuclei were stained with Hoechst 33342 (blue) and membranes were stained with αCD45 (green). **b**, Selective uptake of Cy5-siRNA-loaded αCD4 TsiLNPs by blood CD4 + lymphocytes harvested 1.5 h after intravenous injection and assessed by flow cytometry for Cy5 fluorescence. Red indicates TsiLNP-treated cells; black indicates mock-treated cells. **c**, **d**, αCD4 TsiLNPs loaded with CD45 or luciferase siRNAs were injected on days 1 and 3 and inguinal lymph node lymphocytes were harvested on day 7 and analysed by flow cytometry for CD45 and CD4. Representative dot blots (**c**) and the mean ± s.d. CD45 geometric MFI (**d**) relative to mock-treated cells are shown. Data in **a**–**c** are representative of 3 independent experiments; data in **d** are the mean ± s.d., $n = 3$ biological replicates. ***$P < 0.001$ (two-sided student's t-test).

4 hr incubation in plasma (Supplementary Fig 2c). To construct targeted siRNA-loaded LNPs, which we call TsiLNPs, ASSET and RIg were sequentially added in equimolar amounts to previously described siRNA-loaded LNPs[4,5,12,13]. To verify TsiLNP assembly, we used immunoblotting to probe for ASSET and RIg after high cutoff (1 MDa) dialysis to remove any unbound proteins (Supplementary Fig 3a). RIg only bound if ASSET was incorporated. ASSET-mediated RIg binding was efficient (~98% by protein gel staining) (Supplementary Table 2). This is in contrast to the inefficiency of carbodiimide-mediated chemical conjugation (<0.5%) (Supplementary Fig 3b and Supplementary Table 2). The high RIg binding efficiency led us to explore the possibility of stepwise TsiLNP assembly in which the purification step to remove unbound antibodies could be eliminated. Uptake of αLFA-1 TsiLNPs into TK1 cells was optimal when TsiLNPs were produced using an ASSET:RIg ratio of ~1:1 (Fig. 1i). These data suggest that each RIg bound to one anchored ASSET molecule. Thus, unlike after chemical conjugation, a purification step to remove the unbound antibody (which typically involves gel filtration with large losses) could be omitted.

In contrast to chemically conjugated antibodies, which are randomly oriented so only a fraction is functional, the TsiLNP design assures optimal RIg function as RIg is bound to ASSET through its Fc domain, while the variable domain is exposed for ligand binding. Indeed, αCD34 RIg bound to the LNPs by ASSET maintained its high affinity ($K_d \approx 0.24$ nM by ELISA), whereas the same siRNA-loaded LNPs that were chemically conjugated with RIg (ccTsiLNPs) only bound with an average K_d of ~1.08 nM (measured in three independent conjugations)—a 4.5-fold loss in activity (Fig. 1j and Supplementary Table 2). As ASSET enables controlled mAb orientation we assumed that the mAb Fc domain is shielded to prevent binding and phagocytosis by Fc receptor (FcR)-bearing scavenger cells that are distributed throughout the body. To test this we compared the binding of αCD34 TsiLNPs and ccTsiLNPs to rat FcR that is transiently expressed in HEK293T cells (Fig S3e). αCD34 TsiLNPs did not bind, but the ccTsiLNPs did in three biological replicates (Fig. 1j). Thus, while conjugated LNPs were recognized by rat FcR and therefore vulnerable to clearance by scavenger cells, antibodies bound to TsiLNPs escaped FcR recognition.

We next tested whether TsiLNPs bind to and are taken up by cells bearing the targeted receptor. ASSET-containing LNPs incubated with αLFA-1 RIg were selectively taken up by the LFA-1$^+$ mouse T cell lymphoma cell line TK1. Moreover, TK1 cells did not bind to ASSET LNPs without any antibodies (Supplementary Fig 3c) or to LNPs lacking ASSET (Supplementary Fig 3d). To test the versatility and specificity of TsiLNPs, we assessed mouse macrophage CD44$^+$CD34$^-$ RAW264.7 cell uptake of αCD44 or α CD34 RIg-coated TsiLNPs, incorporating Cy5-labelled siRNAs by immunofluorescence microscopy for ASSET mCherry and Cy5. RAW264.7 uniformly internalized αCD44 (but not αCD34) RIg-coated TsiLNPs (Fig. 2a).

Encouraged by the in vitro results, we next examined whether TsiLNPs cause gene knockdown in targeted cells in vivo. We chose target lymphocytes that are ordinarily hard to transfect and were previously targeted using ccTsiLNPs[4]. Injected αCD4 RIg-coated TsiLNPs, encapsulating Cy5-conjugated siRNAs, were specifically and efficiently taken up by blood CD4+ lymphocytes (Fig. 2b). When CD4 TsiLNPs incorporating CD45 or luciferase control siRNAs were used, CD45 expression was reduced specifically in CD4+ inguinal lymph node lymphocytes. An ~60% reduction of CD45 protein was observed in the silenced population in three independent repeats (Fig. 2c,d). Thus, the TsiLNP platform was able to achieve comparable specific silencing as previously achieved with ccTsiLNPs in CD4+ T cells[4]. The advantage of using the new platform was that this gene knockdown was achieved with negligible calibration using an amount of antibody that was two orders of magnitude lower.

To assess the versatility of the ASSET platform, we next tested whether a simple RIg switch could alter which cells were targeted (Fig. 3a). We compared uptake by blood lymphocytes of TsiLNPs that encapsulate Cy5-conjugated siRNAs and are coated with anti-CD3, CD4, beta7 integrin (Itgb7) or CD25 antibodies (Fig. 3b, and Supplementary Fig 4). Itgb7 is expressed on most T and B lymphocytes as well as on monocytes[14] and CD25 is expressed brightly on regulatory T cells and less brightly on activated T cells. αCD3 TsiLNPs were taken up by both CD4$^+$ and CD4$^-$ CD3$^+$ lymphocytes, but not by CD3$^-$ CD19$^+$ B cells or CD11b$^+$ monocytes. As targeting via αCD3 downregulates CD3 from the cell surface within 1.5 h

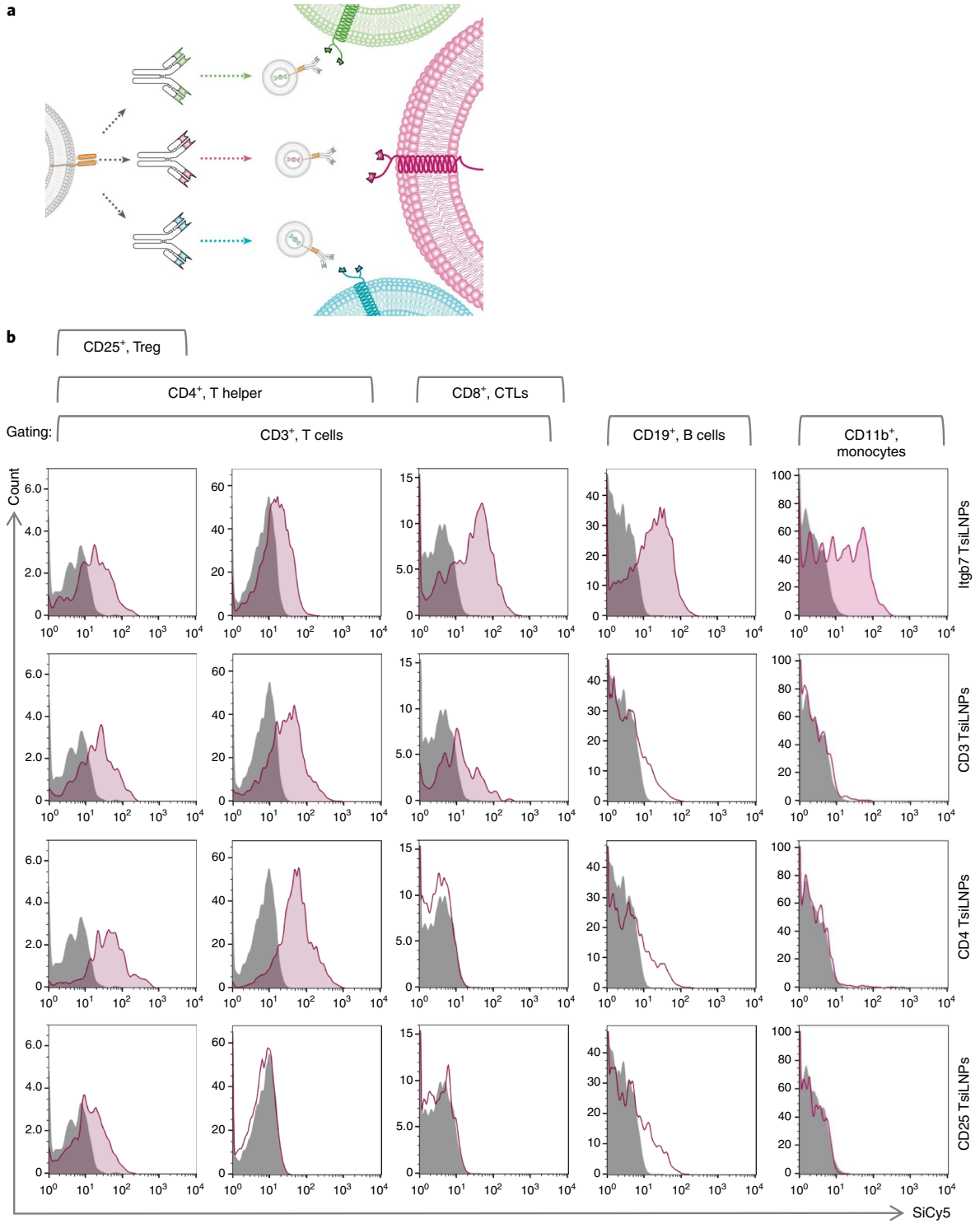

Fig. 3 | In vivo targeting of TsiLNPs. a, Schematic illustration of the versatility of the targeting platform, made possible by coating ASSET-loaded LNPs with diverse RIgs to target different cell subsets. **b**, Cy5-siRNA-loaded TsiLNPs assembled with indicated RIgs (αItgb7, αCD3, αCD4 and αCD25) were injected intravenously and blood leukocytes were isolated 1.5 h after injection and co-stained for CD4, CD3, CD8, CD19, CD11b and CD25. Representative histograms of 3 independent experiments of live mononuclear cells (biological replicates) are shown, gated as indicated. TsiLNPs are shaded red, mock-treated cells in grey.

of TsiLNP administration, we verified specific uptake to $CD4^+$ and $CD8^+$ T cells using CD4 and CD8 labelling (Supplementary Fig 4). CD4 TsiLNPs were uniformly taken up by $CD4^+$ T cells, but not by $CD4^-CD3^+$ T lymphocytes, $CD3^-$ cells or $CD11b^+$ cells. Itgb7 TsiLNPs were taken up by a subset of both $CD3^+$ and $CD3^-$ cells, as expected based on its expression by T and B lymphocytes and monocytes. CD25 TsiLNP uptake was restricted to the small population of $CD25^+$ $CD4^+$ T cells. Thus, simply switching the RIg used for targeting directed LNPs in vivo into cell surface receptor-defined subsets of lymphocytes with precision.

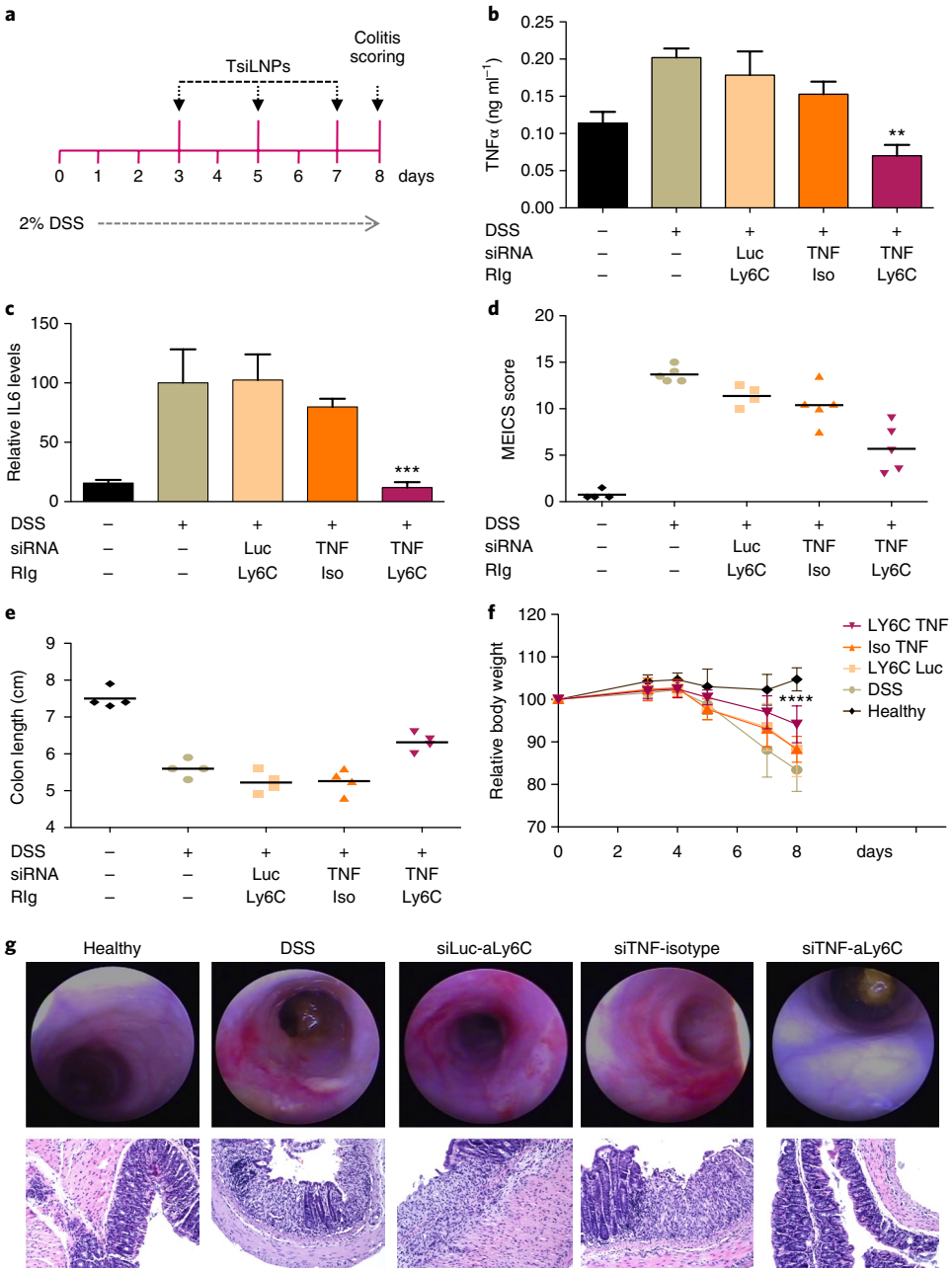

Fig. 4 | TsiLNP-mediated therapeutic gene silencing in a murine colitis model. a, Experimental design. After oral DSS is administered, mice were injected intravenously with αLy6C or isotype control TsiLNPs encapsulating TNF or luciferase siRNAs on days 3, 5, and 7 and were killed on day 8. **b**,**c**, Colonic TNFα (**b**) and IL-6 (**c**) levels in whole tissue lysates were evaluated by ELISA. **d**–**f**, Murine endoscopic index of colitis (MEICS) (**d**) and colon length (**e**) were assessed on day 8 and relative body weight (**f**) was measured daily. Number of mice $n = 4$. Data are mean ± s.d., $n = 5$, $^{*}P < 0.05$, $^{**}P < 0.01$, $^{****}P < 0.0001$ (two-sided Student's *t*-test relative to mice given DSS but not injected with TsiLNPs). **g**, Representative colonoscopy images (top) and histology (hematoxylin and eosin staining, bottom) on day 8. Data in **b**–**g** are representative of 3 independent experiments (as biological replicates).

Next, we tested the potential therapeutic utility of TsiLNPs. Because secretion of TNFα by intestinal macrophages plays a major role in inflammatory bowel disease (IBD), reducing TNFα secretion in the gut should provide protection in an animal model of IBD[15]. For targeting we chose Ly6C, a marker of mouse circulating monocytes and inflammatory tissue macrophages[16,17]. αLy6C TsiLNPs demonstrated 94.2% knockdown by mRNA in vitro in three independent repeats (Supplementary Fig 5a). We next investigated whether TsiLNPs, produced with Cy5-labelled siRNAs and αLy6C RIg, were taken up by Ly6C^{+} blood monocytes (Supplementary Fig 5b,c). Indeed, Ly6C^{+} cells were positive to Cy5 in three mice treated with Ly6C TsiLNPs, but not with control RIg TsiLNPs. Oral administration of the detergent dioctyl sodium sulfosuccinate (DSS) causes colitis in mice and is used as a model of IBD[15]. To assess the therapeutic efficacy of TsiLNPs in this model, Ly6C or control antibody TsiLNPs encapsulating TNF siRNAs were administered intravenously 3, 5 and 7 days after giving DSS, and TNFα knockdown and colitis severity were assessed on day 8 (Fig. 4a). αLy6C TsiLNPs reduced TNFα protein in the large intestine of 5 mice by approximately threefold (Fig. 4b), even below its level in

uninflamed gut. IL-6 expression in the gut, an indicator of inflammation, was also drastically reduced to its baseline levels in healthy mice (Fig. 4c). DSS colitis leads to profound weight loss, a shortening of the inflamed colon and erythema, swelling and inflammatory infiltration of the colon. All of these disease signs were significantly and dramatically reduced in all 5 mice receiving αLy6C TsiLNPs bearing TNF siRNAs (Fig. 4d–g). In contrast, there was minimal or no protection provided by TsiLNPs assembled with isotype control RIg or Luc siRNA. The minimal protection afforded by TsiLNPs assembled with isotype control RIg might be due to their nonspecific phagocytosis by macrophages, which remove particulates. Thus, targeted delivery of TNF siRNAs to Ly6C$^+$ macrophages by TsiLNPs provided protection from DSS colitis.

To test the applicability of TsiLNPs for cancer therapy, we used a model of disseminated bone marrow mantle cell lymphoma (MCL) generated by intravenous injection of a human MCL cell line into immunodeficient mice[5]. Human CD29 RIg was chosen to target these lymphoma cells, and PLK1 was used to cause G2/M cell cycle arrest and then cell death. After verifying that αCD29 TsiLNPs knocked down PLK1 in three biological replicate Granta-519 cells in vitro (Supplementary Fig 6a) and caused cell cycle arrest (Supplementary Fig 6b), we investigated its effect on survival of mice bearing MCL tumours. αCD29 or isotype control antibody TsiLNPs encapsulating PLK1 siRNAs were administered intravenously every 3 days beginning 5 days after tumour cell injection to 10 mice in each group (Supplementary Fig 6c). Mock-treated mice and mice that were treated with TsiLNPs assembled with isotype control RIg had median survival times of 24 and 28 days, respectively, while mice treated with αCD29 TsiLNPs showed prolonged survival for a median of 46 days.

A flexible platform that delivers siRNAs effectively and selectively to targeted cell populations in vivo has tremendous research and therapeutic potential. To translate this platform for human use, an scFv that binds the Fc region of human IgG and humanized IgG should be substituted for the rat reagents. The scFv should have sufficient affinity to avoid exchange with serum IgG. Adapting this flexible platform for human use will enable personal therapy for cancer patients in which the targeted antibody can be adjusted according to each patient's cancer cell surface marker expression. The platform could also allow the use of more than one targeting antibody to reduce the chance of cancer resistance and relapse due to receptor down-modulation.

Here we showed the versatility of this platform for antibody-directed delivery and knockdown in hard-to-transfect immune cells using eight different targeting antibodies (against CD44, CD34, Ly6C, CD3, CD4, CD25, CD29 and Itgb7) and showed its therapeutic effectiveness in a DSS colitis model and in MCL xenografts. Our targeting strategy involves a simple antibody substitution without any recalibration or optimization, which preserves the high affinity of the antibody in the nanoparticle and eliminates its phagocytosis by scavenger cells. This simple approach creates new opportunities to study leukocyte biology in vivo and ultimately might become a novel personalized therapeutic platform to treat leukocyte-related diseases.

Methods

Methods, including statements of data availability and any associated accession codes and references, are available at https://doi.org/10.1038/s41565-017-0043-5.

Received: 8 August 2016; Accepted: 5 December 2017;
Published online: 29 January 2018

References

1. Dahlman, J. E. et al. In vivo endothelial siRNA delivery using polymeric nanoparticles with low molecular weight. *Nat. Nanotechnol.* **9**, 648–655 (2014).
2. McNamara, J. O. II et al. Cell type-specific delivery of siRNAs with aptamer-siRNA chimeras. *Nat. Biotechnol.* **24**, 1005–1015 (2006).
3. Wittrup, A. & Lieberman, J. Knocking down disease: a progress report on siRNA therapeutics. *Nat. Rev. Genet.* **16**, 543–552 (2015).
4. Ramishetti, S. et al. Systemic gene silencing in primary T lymphocytes using targeted lipid nanoparticles. *ACS Nano* **9**, 6706–6716 (2015).
5. Weinstein, S. et al. Harnessing RNAi-based nanomedicines for therapeutic gene silencing in B-cell malignancies. *Proc. Natl Acad. Sci. USA* **113**, E16–E22 (2016).
6. Katakowski, J. A. et al. Delivery of siRNAs to dendritic cells using DEC205-targeted lipid nanoparticles to inhibit immune responses. *Mol. Ther.* **24**, 146–155 (2016).
7. Peer, D., Zhu, P., Carman, C. V., Lieberman, J. & Shimaoka, M. Selective gene silencing in activated leukocytes by targeting siRNAs to the integrin lymphocyte function-associated antigen-1. *Proc. Natl Acad. Sci. USA* **104**, 4095–4100 (2007).
8. Song, E. et al. Antibody mediated in vivo delivery of small interfering RNAs via cell-surface receptors. *Nat. Biotechnol.* **23**, 709–717 (2005).
9. Springer, T. A., Bhattacharya, A., Cardoza, J. T. & Sanchez-Madrid, F. Monoclonal antibodies specific for rat IgG1, IgG2a, and IgG2b subclasses, and kappa chain monotypic and allotypic determinants: reagents for use with rat monoclonal antibodies. *Hybridoma* **1**, 257–273 (1982).
10. Laukkanen, M. L., Teeri, T. T. & Keinanen, K. Lipid-tagged antibodies: bacterial expression and characterization of a lipoprotein-single-chain antibody fusion protein. *Protein Eng.* **6**, 449–454 (1993).
11. de Kruif, J., Storm, G., van Bloois, L. & Logtenberg, T. Biosynthetically lipid-modified human scFv fragments from phage display libraries as targeting molecules for immunoliposomes. *FEBS Lett.* **399**, 232–236 (1996).
12. Semple, S. C. et al. Rational design of cationic lipids for siRNA delivery. *Nat. Biotechnol.* **28**, 172–176 (2010).
13. Cohen, Z. R. et al. Localized RNAi therapeutics of chemoresistant grade IV glioma using hyaluronan-grafted lipid-based nanoparticles. *ACS Nano.* **9**, 1581–1591 (2015).
14. Tiisala, S., Paavonen, T. & Renkonen, R. Alpha E beta 7 and alpha 4 beta 7 integrins associated with intraepithelial and mucosal homing, are expressed on macrophages. *Eur. J. Immunol.* **25**, 411–417 (1995).
15. Peer, D., Park, E. J., Morishita, Y., Carman, C. V. & Shimaoka, M. Systemic leukocyte-directed siRNA delivery revealing cyclin D1 as an anti-inflammatory target. *Science* **319**, 627–630 (2008).
16. Zigmond, E. et al. Ly6C hi monocytes in the inflamed colon give rise to proinflammatory effector cells and migratory antigen-presenting cells. *Immunity* **37**, 1076–1090 (2012).
17. Grainger, J. R. et al. Inflammatory monocytes regulate pathologic responses to commensals during acute gastrointestinal infection. *Nat. Med.* **19**, 713–721 (2013).

Acknowledgements

This work was supported in part by grants from the Dotan Hemato-oncology Center at Tel Aviv University, by The Leona M. and Harry B. Helmsley Nanotechnology Research Fund, by the Kenneth Rainin Foundation and by the ERC grant LeukoTheranostics (number 647410) awarded to D.P.

Author contributions

R.K., N.V. and D.P. conceived and designed the project. R.K., N.V. S.R., M.G., D.R. N.D., L.N., I.H.-H., S.L.-B.-A. and M.H. performed the experimental work. R.K., N.V., M.B., I.B. J.L. and D.P. analysed the data. R.K. N.V. and D.P. wrote the manuscript. All authors discussed the results.

Competing interests

M.B. is an employee of Integrated DNA Technologies, Inc. J.L. is on the Scientific Advisory Board of Alnylam Pharmaceuticals. D.P. declares financial interests in Quiet Therapeutics. The rest of the authors declare no competing financial interests.

Additional information

Supplementary information is available for this paper at https://doi.org/10.1038/s41565-017-0043-5.

Reprints and permissions information is available at www.nature.com/reprints.

Correspondence and requests for materials should be addressed to D.P.

Publisher's note: Springer Nature remains neutral with regard to jurisdictional claims in published maps and institutional affiliations.

Methods

Monoclonal antibodies. RIg αLy6c (clone Monts1, BioXcell)
RIg αItgb7 (clone FIB504, BioXcell)
RIg αCD44 (clone KM81, CEDARLANE)
RIg αCD3 (clone KT3, BioXcell)
RIg αCD4 (clone YTS 177, BioXcell)
RIg αLFA1 antibody (clone M17/4)
RIg αCD25 (clone 280406, R&D Systems)
Isotype RIg (clone 2A3, BioXcell)
RIg αCD45 (clone 30-F11, Biolegend)
RIg αCD19 (clone 6D5, Biolegend)
RIg αCD25 (clone PC61, Biolegend)
RIg αCD11b (clone M1/70, Biolegend)
RIg αCD4 (clone GK1.5, Biolegend)
RIg αCD8 (clone 53.6.7, Biolegend)
RIg αCD3 (clone 145-2C11, Biolegend)
RIg αCD34 (clone mec14.7, a gift from GARLANDA Cecilia, Humanitas Clinical and Research Center)
RIg αCD29 (clone Mab13, BD Pharmingen)

Cell lines. Anti-rat IgG2a hybridoma (ATCC, TIB-173), RAW 264.7 cells (ATCC, TIB-71), HEK293 cells (ATCC, CRL-1573), Tk1 cells (ATCC CRL-2396) and Granta 519 cells (DSMZ, ACC-342) were used. All cells were routinely checked every two months for Mycoplasma contamination using EZ-PCR Mycoplasma Test Kit (Biological Industries) according to the manufacture's protocol.

Anti-rat Ig scFv construction, expression and purification. Total RNA was extracted from hybridoma cells (ATCC, TIB-173) using an EZ-RNA (Biological Industries) reagent and cDNA was synthesized (Quanta Biosciences). Heavy and light IgG chains were cloned as described in a previous study[18]. Anti-rat Ig scFv (scFv) was assembled with an insertion of a $(Gly_4Ser)_3$ linker and cloned into pET22b–pelB vector, downstream of a HexaHisidine tag.

For periplasmic expression, *E. coli Rosetta BL21 (DE3)* cells were transformed with scFv expression vector. When $A_{600nm}=2.5$, 1 mM IPTG was added for 3 h at 30 °C with shaking at 250 r.p.m (1" circular orbit). Periplasmic proteins were extracted according to a standard protocol[19] and scFv was purified using HisTrap HP columns (GE Healthcare Life Science) according to the supplier's recommendations.

ASSET construction, expression and purification. For ASSET engineering we added an NlpA signal peptide and lipidation sequence at the scFv N terminus by a set of PCR reactions. At the scFv C terminus we added the red fluorescent protein mCherry followed by a hexahistidine tag. The DNA sequence was validated by Sanger sequencing. *E. coli* BL21-tuner (DE3) cells were transformed with the ASSET expression vector. When A_{600nm} reached 1, 0.5 mM IPTG was added for induction overnight at 30 °C. ASSET was purified from the membrane fraction and solubilized in 20 mM TRIS(HCL) (pH 8) buffer with 1% Triton X-100 (Sigma-Aldrich), followed by buffer exchange to 1.4% Octyl glucoside (Abcam, ab-142071-50-B) as described previously[10,11] and further purified using HisTrap HP columns (GE Healthcare Life Science). To create micelles, 250 nM cholesterol (Avanti Polar Lipids) was added and ASSET was stored at −80 °C.

ELISA assays. ELISA plates were coated O.N with 5 μg ml^{-1} RIg (BioXcell, clone FIB504) or BSA, for control. After blocking for 2 h at 37 °C with 3% skim milk in PBS, scFv or ASSET were added in serial dilutions for 1 h at room temperature. Mouse αHis (Roche) was used followed by anti-mouse HRP for detection. To test ASSET LNP functionality, the same protocol was followed with an additional step of LNP pre-incubation with 0.2% Triton X-100 (Sigma-Aldrich) for 20 min at 37 °C.

To test TsiLNP and ccTsiLNP RIg functionality, wells were coated overnight with 5 μg ml^{-1} recombinant mouse CD34 (Sino Biological Inc.). After blocking for 2 h at 37 °C with 3% skim milk, TsiLNPs or ccTsiLNPs, pre-incubated with 0.2% Triton X-100 (Sigma-Aldrich), were added in serial dilutions for 1 h at room temperature. αRat HRP was used for detection using TMB solution (Millipore) as substrate and the reaction was stopped by adding 2 M H_2SO_4. Results were analysed by reading A_{450nm} on a plate reader (Biotek).

Endotoxin tests. The Limulus amebocyte lysate (LAL) test was performed by Hy Laboratories Ltd using LAL prepared by the Associates of Cape Cod Inc.

Biacore. The binding affinity of purified mASSET to RIg antibodies was determined by SPR with a Biacore T-200 instrument. mASSET dilutions (0 to 30 nM) in HEPES-buffered saline (HBS) were passed over immobilized RIg on a CM5 sensor chip (about 1,000 resonance units immobilized IgGs). EDC/NHS immobilization was at a flow rate of 20 μl min^{-1}. The dissociation and association constants ($K_{d,a}$) were analysed using Biacore evaluation software 4.1.

siRNAs. Chemically modified siRNAs against CD45, luciferase and luciferase-Cy5 (siCy5) were synthesized at IDT (Coralville) using standard phosphoramidite chemistry and the following sequences.

CD45 siRNA: sense strand:
mCmUrGrGmCmUrGrArAmUmUmUmCrArGrArGmCrAdTsdT anti-sense strand: rUrGrCrUrCrUrGrArArArUrUmCrArGrCmCrArGdTsdT
Luc siRNA: sense strand:
mCmUmUAmCrGmCmUrGrArGmUrAmCmUmUmCrGAdTsdT anti-sense strand: rUrCrGrArArGmUrArCrUmCrArGrCrGmUrArArGdTsdT
TNFα siRNA:
sense strand:
mGmUrCmUrCmArGrCrCrUrCmUrUmCrUmCrAmUrUrCrCrUrGmCT
anti-sense strand:
rArGmCrArGrGrArAmUrGmArGmArArGrArGrGrCrUrGrAmGrAmCmAmU
m:2′-OMe-modified nucleotides. r: RNA bases. phosphorothioate linkages are represented by "s".
PLK1 dsiRNA:
sense strand:
mGmCrUmUrAmArUrGrArCrGmArGmUrUmCrUmUrUrArCrUrUmCT
anti-sense strand:
rArGmArArGrUrArAmArGmArAmCrUrCrGrUrCrArUrUrAmArGmCm AmG

Preparation of LNPs with entrapped siRNAs. LNPs were prepared by Avanti Polar Lipids. Dlin-MC3-DMA (MC3) was synthesized according to a previously described method[13]. Briefly, one volume of lipid mixture (MC3, DSPC, Cholesterol, DMG-PEG, and DSPE-PEG at 50:10.5:38:1.4:0.1 mol ratio) in ethanol and three volumes of siRNA (1:16 w/w siRNA to lipid) in an acetate buffer were injected in to a microfluidic mixing device Nanoassemblr (Precision Nanosystems) at a combined flow rate of 2 ml min^{-1} (0.5 ml min^{-1} for ethanol and 1.5 ml min^{-1} for aqueous buffer). The resultant mixture was dialysed against phosphate buffered saline (PBS) (pH 7.4) for 16 h to remove ethanol. For Cy5-labelled particles, 10% Cy5-labelled non-targeted siRNA was used. To produce LNPs that harbour a functional group for conjugation, DSPE-PEG carboxyl was added to the lipid mixture (MC3, DSPC, Cholesterol, DMG-PEG, and DSPE-PEG carboxyl at 50:10:38:1.5:0.5 mol ratio).

Size distribution. LNP sizes in PBS were measured by dynamic light scattering using a Malvern nano-ZS Zetasizer (Malvern Instruments Ltd).

Transmission electron microscopy. A drop of aqueous solution containing LNPs or ASSET LNPs was placed on a carbon-coated copper grid and dried and analysed using a JEOL 1200 EX transmission electron microscope.

ASSET LNP incorporation and TsiLNP assembly. To incorporate ASSET into LNPs, ASSET was incubated with LNPs for 48 h at 4 °C (1:36, ASSET:siRNA weight ratio).To test incorporation efficiency, TsiLNPs were separated from free ASSET by dialysis using a 1 MDa cutoff membrane (Biolab Ltd). ASSET incorporation was measured by mCherry fluorescence and ELISA. To construct TsiLNPs, RIg was incubated with ASSET LNPs for 30 min (1:1, RIg:ASSET weight ratio). Free RIg was removed by dialysis with a 1 MDa cutoff membrane. LNP components were detected by western blot. ASSET was detected using αHis tag antibody (Roche) followed by HRP-conjugated goat anti-mouse antibody. RIg was detected by HRP-conjugated goat anti-Rat antibody. After optimizing the RIg:ASSET ratio, it was not necessary to remove unbound RIg as all of the RIg was bound.

siRNA entrapment efficiency and plasma stability. The efficiency of siRNA encapsulation was determined by agarose gel electrophoresis as previously described[13]. Briefly, the encapsulation efficiency was determined by comparing Ethidium bromide siRNA staining of LNPs and ASSET LNPs in the presence or absence of 0.2% Triton X-100 (Sigma-Aldrich). To test TsiLNP siRNA stability in plasma, TsiLNPs were incubated in murine plasma for 0–240 min at 37 °C and then siRNA integrity was tested by agarose gel electrophoresis. Densitometry analysis was performed using Image.

LNP quantification. To quantify LNPs after conjugation or after the ASSET assembly procedure, Quant-iT RiboGreen RNA assay (Life Technology) was used as previously described[13]. 2 μl of LNPs or dilutions of siRNA at known concentrations were diluted in a final volume of 100 μl of TE buffer (10 mM Tris-HCl, 20 mM EDTA) and 0.5% Triton X-100 (Sigma-Aldrich) in a 96-well fluorescent plate (Costar, Corning). The plate was incubated for 10 min at 40 °C to allow particles to become permeabilized before adding 99 μl of TE buffer and 1 μl of RiboGreen reagent to each well. Plates were shaken at room temperature for 5 min and fluorescence (excitation wavelength 485nm, emission wavelength 528 nm) was measured using a plate reader (Biotek).

Confocal microscopy. RAW 264.7 cells (ATCC, TIB-71) were incubated for 30 min at 37 °C with TsiLNPs, self-assembled with αCD44 RIg (CEDARLANE) or without before staining with Hoechst 33342 (Sigma Aldrich) and αCD45. Cells were washed, and images were analysed using a Nikon C2 (Nikon Instruments Inc.) confocal microscope.

Preparation of antibody-conjugated LNPs. To conjugate the αCD34 antibody (clone mec14.7, GARLANDA Cecilia, Humanitas Clinical and Research Center) to carboxyl functionalized LNPs, EDC, NHS, LNPs and αCD34 RIg were combined for 3 h at room temperature followed by overnight incubation at 4 °C. To remove free αCD34, conjugated particles were loaded on a Cl4b column. Particle-containing fractions were combined and concentrated with an Amicon 100 kDa cutoff filter (Millipore).

Targeted LNP interaction with Fc receptor. HEK293T cells (ATCC, CRL-1573) were co-transfected with Fcgr2a (CD32) expression plasmids and GFP reporter plasmids using Lipofectamine 2000 (Thermo Fisher Scientific) following the manufacturer's protocol; 48 h after transfection, cells were harvested and treated with 1 μg of siCy5-loaded LNPs, conjugated to αCD34 (ccTsiLNPs) or 1 μg of siCy5 entrapped within TsiLNPs and self-assembled with αCD34 RIg. As a control, cells were also treated with 1 μg siCy5-loaded naked LNPs. Cy5 and GFP fluorescence was analysed by flow cytometry (Becton Dickinson FACScalibur). To measure LNP interactions with Fc receptors, Cy5 levels were measured on GFP high cells, representing highly transfected cells and GFP negative cells, representing untransfected cells. The score for interaction was calculated as the ratio of geometric mean Cy5 fluorescence intensity of GFP high and GFP negative cells.

Optimization of ASSET:RIg ratio. ASSET LNPs encapsulating siCy5 were incubated for 10 min with increasing amounts of αLFA1 (clone M17/4) RIg (0–5:1, RIg:ASSET molar ratio). siCy5-loaded TsiLNPs (1 μg RNA) were incubated with TK1 cells for 15 min at 4 °C in DMEM (Biological Industries) supplemented with 10% serum. LNP binding was detected by measuring the Cy5 fluorescence of encapsulated Cy5siRNA by flow cytometry.

Animal experiments. All animal protocols were approved by Tel Aviv University Institutional Animal Care and Usage Committee and in accordance with current regulations and standards of the Israel Ministry of Health. All animal experiments were conducted in a double blinded fashion; the researchers were blinded to group allocation and administered treatments. Mice were randomly divided in a blinded fashion in the beginning of each experiment.

In vivo uptake and silencing by TsiLNPs. Ten-week-old female C57BL6/J mice were obtained from Harlan Laboratories. To measure cell-specific LNP uptake, mice were injected intravenously with siCy5-loaded TsiLNPs, self-assembled with the following RIgs: αItgb7, αCD3, αCD4 (BioXcell) and αCD25 (R&D Systems). Leukocytes were isolated by density centrifugation using Ficoll-paque Plus (GE Healthcare) from heparinized blood collected 1.5 h after injection. Cells in PBS containing 1% fetal bovine serum (Biological Industries) were stained with fluorescently labelled αCD4, αCD8, αCD3, αCD19, αCD11b and αCD25 antibodies (BioLegend) for 30 min at 4 °C and analysed by flow cytometry. To measure gene knockdown, TsiLNPs self-assembled with αCD4 RIg containing CD45 or luciferase siRNA were injected intravenously on day 1 and day 3 (3 mg kg^{-1}). On day 5, inguinal lymph nodes were isolated and minced to make a single-cell suspension. Cells were washed twice with PBS, passed through a 70 μm cell strainer and stained in PBS containing 1% fetal bovine serum with fluorescently labelled αCD4, CD3 and CD45 antibodies (BioLegend) for 30 min at 4 °C. Cells were analysed on a Becton Dickinson FACScalibur flow cytometer with CellQuest software (Becton Dickinson). Data analysis was performed using FlowJo software (Tree Star, Inc.).

In vitro knockdown. RAW 264.7 cells (ATCC, TIB-71) (60% confluence) in 24-well plates were treated with 0.5 μg of siTNFα or siLuc entrapped in LNPs. After 16 h, cells were washed and activated with 2.5 ng ml^{-1} IFNχ (Peprotech). After 48 h, cells were harvested and mRNA was isolated using EZ-RNA (Biological Industries), and cDNA was prepared using a cDNA synthesis kit (Quanta Biosciences). *Gapdh* was used as the endogenous control. The following sequences were used for qRT-PCR, normalized to mouse *Gapdh*: *Gapdh* Fwd: 5′ TTG TGG AAG GGC TCA TGA CC 3′; Rev: 5′ TCT TCT GGG TGG CAG TGA TG 3′; *TNF* Fwd: 5′ GCA CCA CCA TCA AGG ACT CAA 3′; Rev: 5′ TCG AGG CTC CAG TGA ATT CG 3′.

Granta 519 cells (0.3×10^6) were placed in tissue culture 24-well plates with 0.5 ml of full medium. αCD29-TsiLNPs-dsPLK1 or αCD29-TsiLNPs-siLuc were added to the wells (8 μg ml^{-1}). Sixty hours following initial exposure to treatments, cells were harvested for mRNA quantification and cell cycle analysis. Human *eLF3a* was used as the PCR normalization control. Primer sequences: *eLF3a* Fwd: 5′ TCC AGA GAG CCA GTC CAT 3′, *eLF3a* Rev: 5′ CCT GCC ACA ATT CCA TGC T 3′. *PLK1* Fwd: 5′ ACC AGC ACG TCG TAG GAT TC 3′. *PLK1* Rev: 5′ CAA GCA CAA TTT GCC GTA GG 3′

Cell cycle studies. Granta 519 transfected cells were washed with ice-cold PBS and fixed with 70% ethanol for 1 h. After washing twice with cold PBS, cells were incubated for 10 min at 37 °C in 250 μl PBS with 10 μg ml^{-1} propidium iodide (PI), 0.1 mg ml^{-1} DNase-free RNase A (Sigma) and 0.01% Triton-X. PI fluorescence was assessed by flow cytometry. Analyses by FlowJo were performed on at least 9,000 cells per sample after gating out debris and cell doublets based on FL2-Area/FL2-Width channels. Cell cycle distributions were obtained via the application of the Dean–Jett–Fox model on gated cells with root mean square scores ranging between 1.5 and 2.5.

IBD model. Colitis was induced in 10-week-old female C57BL/6 mice (Harlan laboratories) using dextran sodium sulphate (DSS) as previously described[15]. Mice were fed for 8 days with 2% (wt/vol) DSS in the drinking water. Suspensions (200 μl in PBS) of TsiLNPs loaded with 1 mg kg^{-1} siRNAs against TNF or Luciferase and self-assembled with αLy6C or isotype control RIg (BioXcell) were injected intravenously on days 3, 5 and 7. Body weight was monitored every other day. On day 8 colitis severity was assessed by colonoscopy scored using the Murine Endoscopic Index of Colitis (MEICS) and then the mice were killed. All MEICS scoring was determined based on three impartial assessments. The length of the entire colon from cecum to anus was measured. Small segments of the colon were taken for histologic and immunohistochemistry evaluation. Colon samples were homogenized to assess cytokines by IL-6 and TNFα ELISA kits (R&D Systems).

MCL xenograft model. Eight-week-old female C.B-17/IcrHsd-Prkdc scid mice ($n = 10$ per group) were treated, beginning 5 days after intravenous injection of 2.5×10^6 Grant 519 cells as described[5], with PBS (mock), isotype control RIg-LNP-siPLK1 or αCD29-LNP-siPLK1. LNPs containing 2 mg kg^{-1} siRNA were injected retro-orbitally on days 5, 8, 12, 15, 19, 22 and 26 after tumour injection. The response was assessed by survival. Mice that lost 15% of their body weight or developed limb paralysis were euthanized.

Statistical analysis. All data are expressed as mean ± s.d. Statistical analysis for comparing two experimental groups was performed using two-sided Student's *t*-tests. In experiments with multiple groups, one-way ANOVA with a Bonferroni correction was used. Kaplan–Meier curves were used to analyse survival. A value of $P < 0.05$ was considered statistically significant. Analyses were performed with Prism 7 (Graph pad Software). Differences are labelled n.s. for not significant, * for $P \leq 0.05$, ** for $P \leq 0.01$, *** for $P \leq 0.001$ and **** for $P \leq 0.0001$. The sample size of each experiment was determined to be the minimal necessary for statistical significance by the common practice in the field. The similarity between the variances of each statistically compared group was verified by *F* tests. Pre-established criteria for the removal of animals from experiment were based on animal health, behaviour and well-being as required by ethical guidelines; no animals were excluded from the experiments.

Data availability. All relevant data are available from the authors upon reasonable request.

References

18. Benhar, I. & Pastan, I. Cloning, expression and characterization of the Fv fragments of the anti-carbohydrate mAbs Bl and B5 as single-chain immunotoxins. *Protein Eng.* **7**, 1509–1515 (1994).
19. Vaks, L. & Benhar, I. Production of stabilized scFv antibody fragments in the *E. coli* bacterial cytoplasm. *Methods Mol. Biol.* **1060**, 171–184 (2014).